Combining Atom Transfer Radical Polymerization and Melt Compounding for Producing PMMA/Clay Nanocomposites

D. Lerari,[1,2] S. Peeterbroeck,[3] S. Benali,[4] A. Benaboura,[1] Ph. Dubois[3,4]

[1]*Faculté de Chimie, Laboratoire de Synthèse Macromoléculaire et Thio-organique Macromoléculaire, Université des Sciences et de la Technologie Houari Boumediene, B.P 32 El-alia, 16111 Bab-ezzouar, Alger, Algeria*
[2]*Centre de Recherche Scientifique et Technique en Analyse Physico-chimiques (CRAPC), B.P 248, Alger RP 16004, Algeria*
[3]*Materia Nova asbl, Parc Initialis, Avenue N. Copernic 1, B-7000 Mons, Belgium*
[4]*Center of Innovation and Research in Materials and Polymers CIRMAP, Laboratory of Polymer and Composite Materials, University of Mons—UMONS, Place du Parc 23, B-7000 Mons, Belgium*

Received 5 April 2010; accepted 27 September 2010
DOI 10.1002/app.33549
Published online 3 March 2011 in Wiley Online Library (wileyonlinelibrary.com).

ABSTRACT: Nanocomposites based on poly (methyl methacrylate) (PMMA) and 3 wt % of clay (montomorillonite) organomodified with alkylammonium cations bearing alkyl halide function (OCTANBr^{i}BBr-CL) have been obtained by melt blending. The "nanohybrid" masterbatch approach, already used within other matrices, has also been tested to produce this type of material. Accordingly, highly filled ($\sim$ 30 wt %) PMMA-OCTAN-Br^{i}BBr-CL nanohybrid has been synthesized by atom transfer radical polymerization (ATRP) of MMA as *in situ* initiated from the alkyl halide functions decorating the nanoclay surface. This nanohybrid, i.e., PMMA-grafted organomodified clay, has been added as masterbatch and melt-blended within commercial PMMA. A significantly better clay nanoplatelet dispersion of the samples prepared via the masterbatch process was evidenced by wide-angle X-ray diffraction (WAXD) and transmission electron microscopy (TEM). As a result, these exfoliated nanocomposites proved to be characterized by better thermal and mechanical properties than the more conventional physical blends, as evidenced by thermogravimetrical analysis (TGA) and dynamical mechanical analysis (DMTA), respectively. © 2011 Wiley Periodicals, Inc. J Appl Polym Sci 121: 1355–1364, 2011

Key words: poly (methyl methacrylate); clay; nanocomposites; grafting; ATRP polymerization; masterbatch

INTRODUCTION

Poly(methyl methacrylate) (PMMA) exhibits several interesting properties, combining excellent optical characteristics (clarity, transparency from near UV to near IR), thermal stability, mechanical and electrical properties, weather resistance, and easy shaping. Accordingly, PMMA-based materials currently find applications in many technological and productive fields.[1–7] However, PMMA is still suffering from some drawbacks, e.g., in terms of barrier properties but also scratch (abrasive) resistance, limiting their use in some specific areas.

The reinforcement of polymeric materials with a few weight percent of nanoparticles (layered-silicate clay, carbon nanotubes, metallic oxides, or others) is known to generate nanocomposites, which can display significantly improved properties in comparison with those of the neat polymers at least when the nanofillers can be finely distributed/dispersed throughout the matrix. Likely montmorillonite (MMT) represents the most used layered silicate for the preparation of polymer–clay nanocomposites.[8–13] Most of the time, the nanoplatelet surface of this natural clay has to be organically modified to reduce its hydrophilic character and ensure affinity with the organophilic polymer chains. This polymer–clay compatibility is often established by cation exchange reaction between sodium cations, initially existing in the silicate interlayer spacing and an alkylammonium (or phosphonium) salt.[14–19] The preparation methods also contribute to the resultant nanocomposite structure with two extreme morphologies, i.e., simple clay intercalation and complete exfoliation/delamination of the nanoplatelets.

Correspondence to: D. Lerari (lerari_zinai@yahoo.fr) or Ph. Dubois (philippe.dubois@umons.ac.be)

Contract grant sponsor: Belgian Federal Science Policy Office; contract grant number: SSTC-PAI 6/27.
Contract grant sponsor: Région Wallonne (Program of Excellence "OPTI^{2}MAT").

As far as PMMA/layered-silicate nanocomposites are concerned, many studies have been reported, often employing traditional methods known for preparing nanocomposites such as *in situ* intercalative polymerization (either in emulsion or in bulk)[20–25] and melt blending processes.[26–29] Recently, a new approach has been investigated to enhance the clay nanoplatelet delamination within the nanocomposite materials, the so-called "reactive masterbatch" process. It essentially consists of surface-grafting polymer chains miscible with the polymer matrix onto the clay nanoplatelets to compatibilize the clay/matrix interface and to facilitate the homogeneous dispersion of the nanofillers. This technique is often based on "grafting-from" intercalative polymerization,[30] followed by dispersion of the resulting polymer surface-treated clay (actually used as "masterbatch") in the polymer matrix via conventional melt-mixing processes. Interestingly, this masterbatch technique involving poly(ε-caprolactone) (PCL) as surface-grafted polymeric compatibilizer proved very efficient for dispersing organomodified MMT within chlorinated polyethylene (CPE),[31–33] poly(styrene-*co*-acrylonitrile) (SAN),[34,35] poly(vinyl chloride) (PVC),[36] and other polyester matrices[37–39] yielding nanocomposite materials displaying performances significantly improved when compared to more conventional melt-blends.

The present work aims at focusing on high-performance PMMA-clay nanocomposites as produced via the aforementioned "masterbatch" approach. Purposely, polymer-grafting reaction via atom transfer radical polymerization (ATRP) and melt-blending process have been combined with each other. Commercial pristine MMT, i.e., Cloisite®Na (Na-CL) has been first organically modified with [2-(2-bromo-2-methyl-propionyloxy)-ethyl]-dimethyl-octadecyl-ammonium bromide (OCTANBr^{i}BBr) to produce a modified nanoclay decored by halogenated alkyl species all along the nanoplatelet surface (OCTANBr^{i}BBr-CL). This bromo-functionalized ammonium was then involved as an initiator in the catalyzed ATRP of MMA monomer yielding PMMA-grafted organoclay nanohybrids (PMMA-OCTANBr^{i}BBr-CL). These nanobybrids (still containing a high content in clay) were finally dispersed in PMMA matrix in the melt state, leading to PMMA/PMMA-OCTANBr^{i}BBr-CL nanocomposites containing 3 wt % of inorganics.

To highlight the interest of using this "masterbatch" technique, other PMMA-based compositions (with the same final content of 3 wt % of inorganics) have been prepared directly with the organoclay OCTANBr^{i}BBr-CL, thus without any polymer chain grafting. The morphology, thermal, and thermomechanical properties of the resulting (nano)composites have been investigated by wide-angle X-ray diffraction (WAXD), transmission electron microscopy (TEM), thermogravimetrical analysis (TGA), and dynamical mechanical analysis (DMTA).

EXPERIMENTAL

Materials

Methyl methacrylate (MMA, 99% from Aldrich) was passed through a column of basic alumina (Aldrich) to remove the stabilizer (inhibitor), dried over calcium hydride (CaH_2, 98% Aldrich) for 24 h, and distilled under reduced pressure prior to use. Triethylamine (NEt_3, 99% from Aldrich) was dried over barium oxide (BaO, 98% Aldrich) for 24 h and distilled under reduced pressure before use. *N,N*-dimethylethanolamine (from Chem-Lab), 1-bromooctadecane (from Sigma Aldrich), 2-bromoisobutyryl bromide (98% from Aldrich), magnesium sulfate (99%, from Aldrich), sodium hydrogenocarbonate (99%, from Aldrich), copper bromide (98% from Fluka), and 1,1,4,7,10,10-hexamethyltriethylenetramine (HMTETA, 97%, from Aldrich) were used as received without further purification. Commercial grade PMMA (Plexiglas®8*N*, M_n = 100,000 g/mol) was supplied by Evonik. Cloisite®Na (CLNa), a sodium MMT, was supplied by Southern Clay Products.

Synthesis of octadecyldimethyl hydroxyethyl ammonium bromide (OCTANBrOH) (3)

The octadecyldimethyl hydroxyethyl ammonium bromide was synthesized by a substitution reaction of *N,N*-dimethylethanolamine on 1-bromooctadecane, as described elsewhere.[40]

Synthesis of the ATRP initiator [2-(2-bromo-2-methyl-propionyloxy)-ethyl]-dimethyl-octadecyl-ammonium bromide (OCTANBr^{i}BBr) (5)

To a solution of octadecyldimethyl hydroxyethyl ammonium bromide (OCTANBrOH) **(3)** (5 g, 12 mmol) in chloroform (15 mL), triethylamine was added (3 mL, 25 mmol) followed by an excess of 2-bromoisobutyryl bromide (3 mL, 24 mmol). The solution was stirred for 24 h at room temperature (Scheme 1). To ensure the complete conversion of the hydroxyl groups, the temperature was increased and maintained at 40°C for 2 h. The solution was washed first with distilled water and then with saturated sodium hydrogenocarbonate solution. The organic layer was isolated and dried over magnesium sulfate, filtered off, and the solvent removed under vacuum to give the desired product, noted as OCTANBr^{i}BBr (yield: 80%).

^{1}H-NMR (300 MHz, $CDCl_3$) δ: 0.88 ppm (t, —CH_3), 1.24–1.35 ppm (s, —$(CH_2)_{15}$—), 1.78 ppm

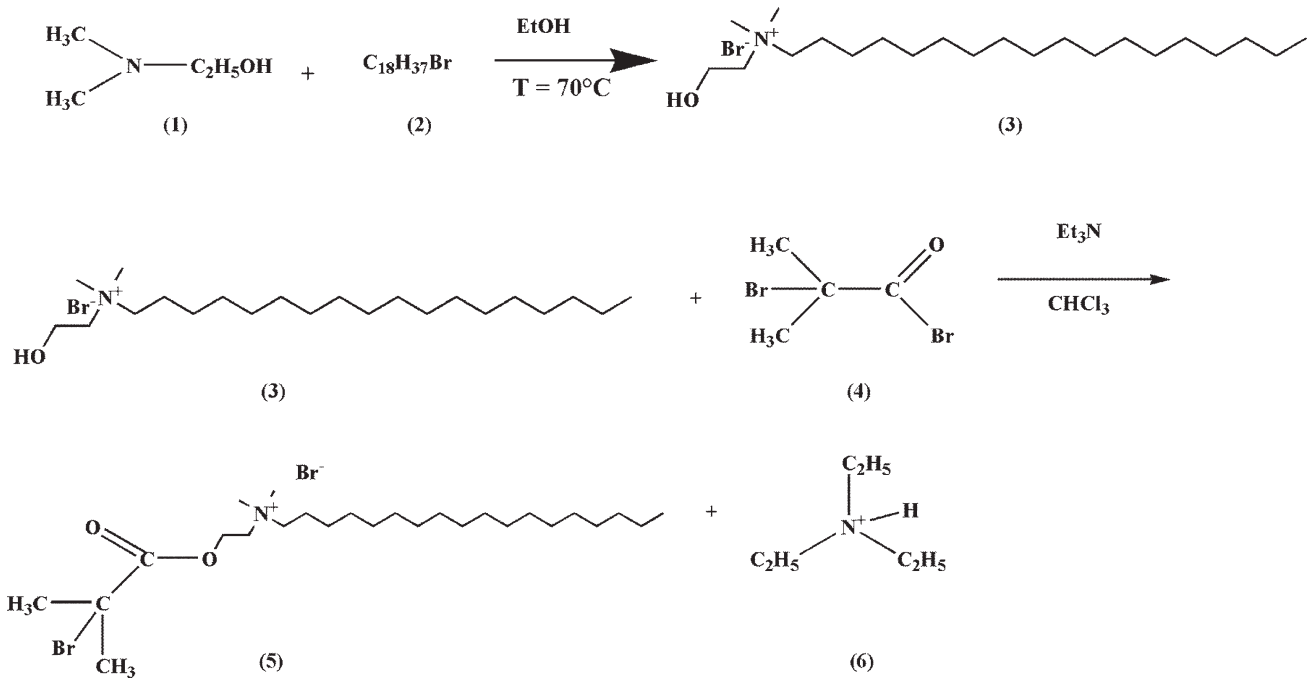

Scheme 1 Three-step synthesis of the [2-(2-bromo-2-methyl-propionyloxy)-ethyl]-dimethyl-octadecyl-ammonium bromide (OCTANBr^{i}BBr) **(5)**.

(s, N—CH_2—CH_2—), 1.95ppm (s, CO—C—CH_3), 3.49 ppm (s, $(CH_3)_2N$), 3.63 ppm (m, —N—CH_2—CH_2—), 4.22 ppm (m, —N—CH_2—CH_2O—), 4.69 ppm (m, —CH_2—O—).

Organo-modification of Cloisite®Na (CLNa) with ATRP initiator (5)

Pristine clay (CLNa) was swollen in water at 80°C for 2 h upon agitation (mixing rate 400 rpm). The ammonium bromide (1.5 equiv of ammonium/Na^+) was dissolved in water at 60°C and added to the clay suspension under agitation. After one night at 80°C, the mixture was filtered off and the collected organoclay was washed with hot water to eliminate the excess of ammonium bromide and sodium ions, and finally freeze-dried for about 24 h. The obtained organomodified MMT was noted as **OCTANBr^{i}BBr-CL**.

Preparation of PMMA/clay nanohybrids by controlled radical polymerization

The preparation of PMMA-OCTANBr^{i}BBr-CL nanohybrid is based on *in situ* ATRP of MMA initiated by bromide groups of the alkyl ammonium cations (OCTANBr^{i}BBr) covering the clay layer, as illustrated in Scheme 2. All experiments were performed under inert atmosphere and the best conditions are mentioned hereafter. The organoclay (2.2 g) was introduced in a glass reactor equipped with a three-way stopcock and then dispersed in toluene (24 mL) for one night. Cu(I)Br (12.2 mmol) and HMTETA (24.4 mmol) were transferred simultaneously into the glass reactor by using a previously flame-dried stainless steel cannula. Freshly distilled monomer (49 mmol), bubbled with nitrogen was transferred into the glass reactor. The reactor was subsequently heated up to 80°C for 4 h and then stopped by cooling down the glass reactor in liquid nitrogen. The resulting composite was purified by precipitation in cold heptane to remove the residual monomer, followed by dissolution in THF and precipitation in distilled water to remove copper residues. The obtained masterbatch was dried under vacuum until a constant weight was obtained (yield: 87%). The inorganic content (31 wt %) of the recovered PMMA-OCTANBr^{i}BBr-CL nanohybrid was determined by TGA.

To confirm the efficient PMMA chain grafting onto the organomodified MMT, three samples containing equal quantities of organomodified clay, namely the organomodified clay (OCTANBr^{i}BBr-CL) alone (vial 1), the PMMA/OCTANBr^{i}BBr-CL simple blend (vial 2), and the PMMA/PMMA-OCTANBr^{i}BBr-CL "grafted" nanocomposite (vial 3) have been stirred in chloroform at room temperature. After centrifugation at 4000 rpm for 30 min, the supernatants were collected. Figure 1 shows the chloroform extracts (supernatants) as obtained from the organomodified clay and the two nanocomposite samples. The supernatant was totally

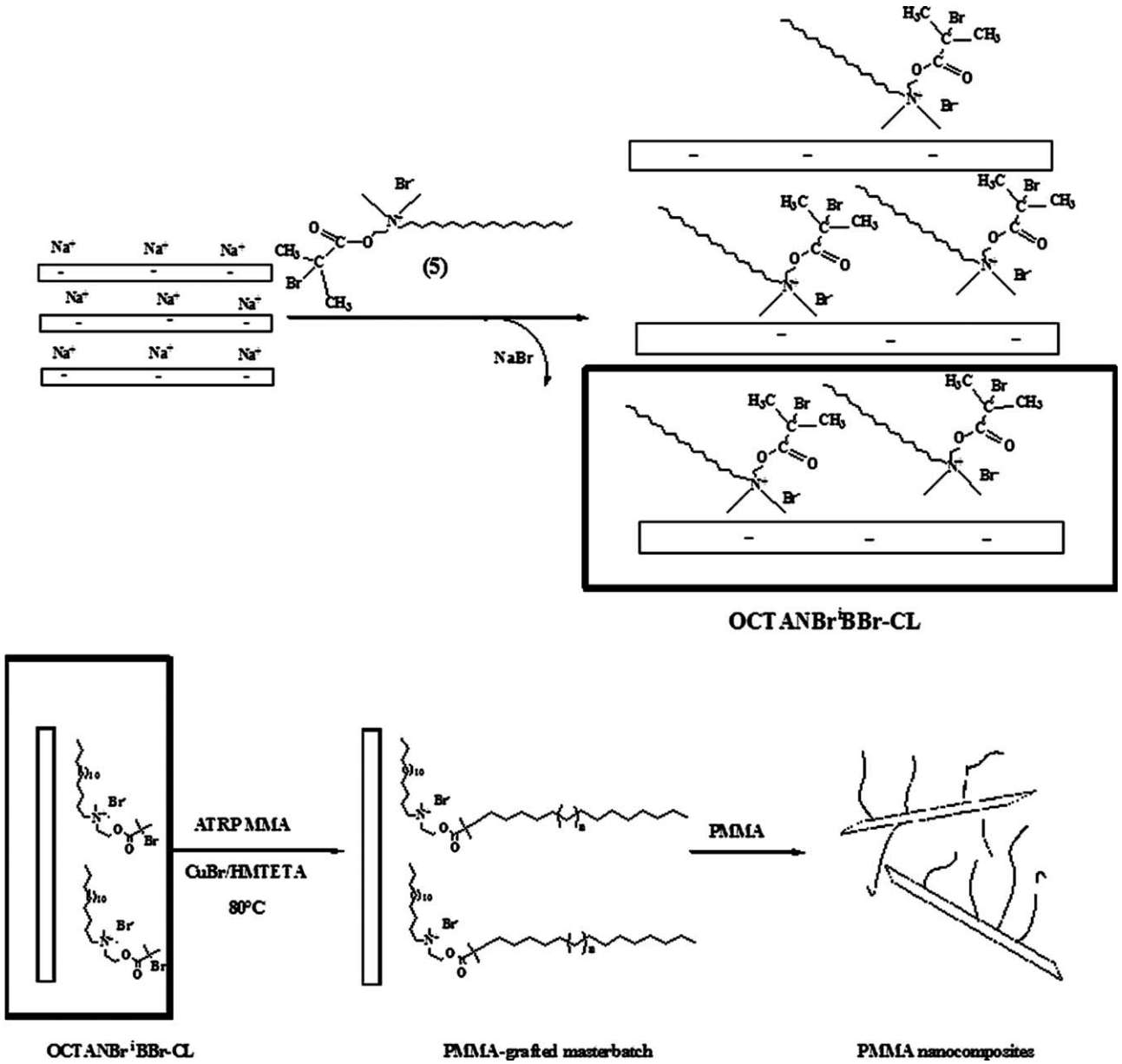

Scheme 2 Sketch for the synthetic pathway used to prepare PMMA–organoclay nanocomposites via the masterbach process.

transparent in the case of both the organomodified clay (vial 1) and the PMMA/organomodified clay blend (vial 2) because of lack of interaction between the inorganic and polymeric components. In opposition, the supernatant in the vial 3 corresponding to the masterbatch-based nanocomposite shows coloration and turbidity attesting for the presence of organomodified clay maintained in suspension via the grafted PMMA chains. These grafted chains are solvated by chloroform, a good solvent for PMMA, preventing the complete sedimentation of the nanoplatelets during the centrifugation step. Such a qualitative observation fully attests for the efficiency of the grafting/polymerization as initiated from the organomodified clay surface. However it is worth noting that this permanent grafting does not allow for the PMMA molecular weight characterization by, e.g., size exclusion chromatography (SEC)

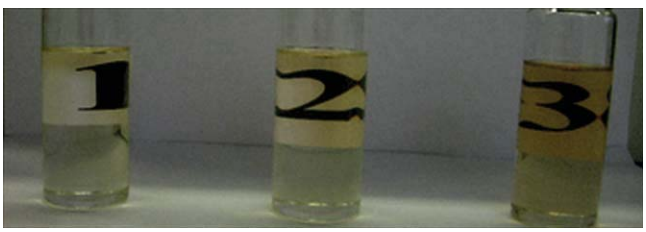

Figure 1 Chloroform extracts (supernatants) of OCTANBriBBr-CL (1), PMMA/OCTANBr^{i}BBr-CL (2), and PMMA/PMMA-OCTANBr^{i}BBr-CL (3) after centrifugation. [Color figure can be viewed in the online issue, which is available at wileyonlinelibrary.com.]

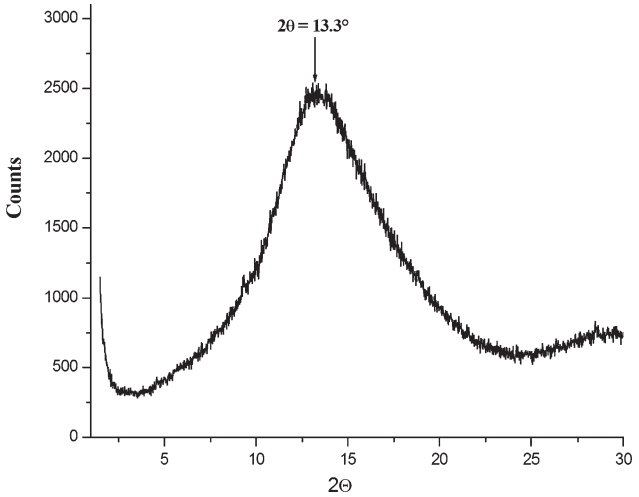

Figure 2 Characteristic XRD pattern of Plexiglas® 8N PMMA.

For sake of comparison, ATRP of MMA was also initiated from OCTANBr^{i}BBr in the absence of clay and under the same experimental conditions. Interestingly enough, the recovered "free" PMMA chains could be analyzed by SEC attesting for a control over the polymerization reaction and the polymer molecular parameters (M_w:18,000 g/mol, $M_w/M_n = 1.19$).

Preparation of nanocomposites by melt blending process

The nanocomposites containing 3 wt % of inorganics were prepared by melt blending commercial grade PMMA with either OCTANBr^{i}BBr-CL or PMMA-OCTANBr^{i}BBr-CL nanohybrid in a twin-screw mini extruder Thermo Haake following well-defined operating conditions, i.e., at 230°C for 8 min (at 80 rpm). The collected samples were then compression-molded to obtain 3-mm thick plates. For the sake of comparison, the unfilled PMMA matrix was also processed under the same conditions.

Characterization

WAXD patterns were recorded with a Siemens D5000 diffractometer using the Cu K_α radiation ($\lambda = 0.15406$ nm). The data were recorded from 1.65° to 30° by step of 0.04° and scanning rate of 10°/min, generator tension was 40 kV and the current was 50 mA. TEM micrographs were obtained with a Philips CM200 electron microscope using an acceleration voltage of 120 kV. The samples were ~ 50 nm thick and prepared by ultracryomicrotome cutting at −100°C with a diamond knife. TGA was performed under air flow (69 cm^3/min) and helium flow (74 cm^3/min) using a TA Instruments Q50 apparatus with a heating rate of 20 K/min from ambient temperature to 800°C. DMTA were performed with a DMTA 2980 from TA instrument in the temperature range of 20°C–200°C with a heating rate of 3 K/min in the dual cantilever mode at 1 Hz with a deformation amplitude of 15 μm. Measurements were carried out on 50 × 12 × 2 mm^3 compression-molded samples. Fire behavior qualitative test were performed on 50 × 12 × 2 mm^3 compression-molded plates of PMMA and PMMA/PMMA-OCTANBr^{i}BBr-CL nanocomposite. Samples were simultaneously ignited from one extremity to determine the time of combustion.

RESULTS AND DISCUSSION

Morphology

(Nano)composites obtained by simple melt blending

The amorphous thermoplastic PMMA matrix used in this study is a commercial formulation named Plexiglas®*8N*. Therefore, a morphological characterization by XRD of virgin PMMA has been first carried out after processing in the mini-extruder under the preparation conditions used for processing the nanocomposites. The XRD pattern of PMMA presented in Figure 2 only shows a very broad peak centered at $2\theta = 13.3°$. The (nano)composites prepared by simple melt blending have been also characterized by XRD. The basal spacing d_{001} of the nanocomposites was determined from the 2θ position of the (001) diffraction peak using Bragg's equation ($n\lambda = 2d\sin\theta$, where n is an integer determined by the order given, λ is the wavelength of X-rays, d is the spacing between the planes in the atomic lattice, and θ the angle between the incident ray and the scattering planes).[10] The obtained XRD patterns are presented in Figure 3. The (001) plane peak of the clay shifts toward lower values of 2θ angle after replacement of the Na^+ ions by the organic modifier. The diffraction peak of PMMA/OCTANBr^{i}BBr-CL is

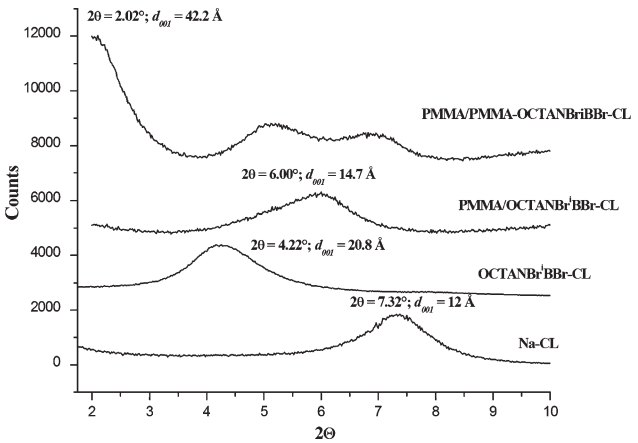

Figure 3 XRD patterns for OCTANBr^{i}BBr-CL, PMMA/OCTANBr^{i}BBr-CL, and PMMA/PMMA-OCTANBr^{i}BBr-CL nanocomposites (3 wt % of inorganics). (Inset number denotes the interlayer distance (d_{001}) of organoclay).

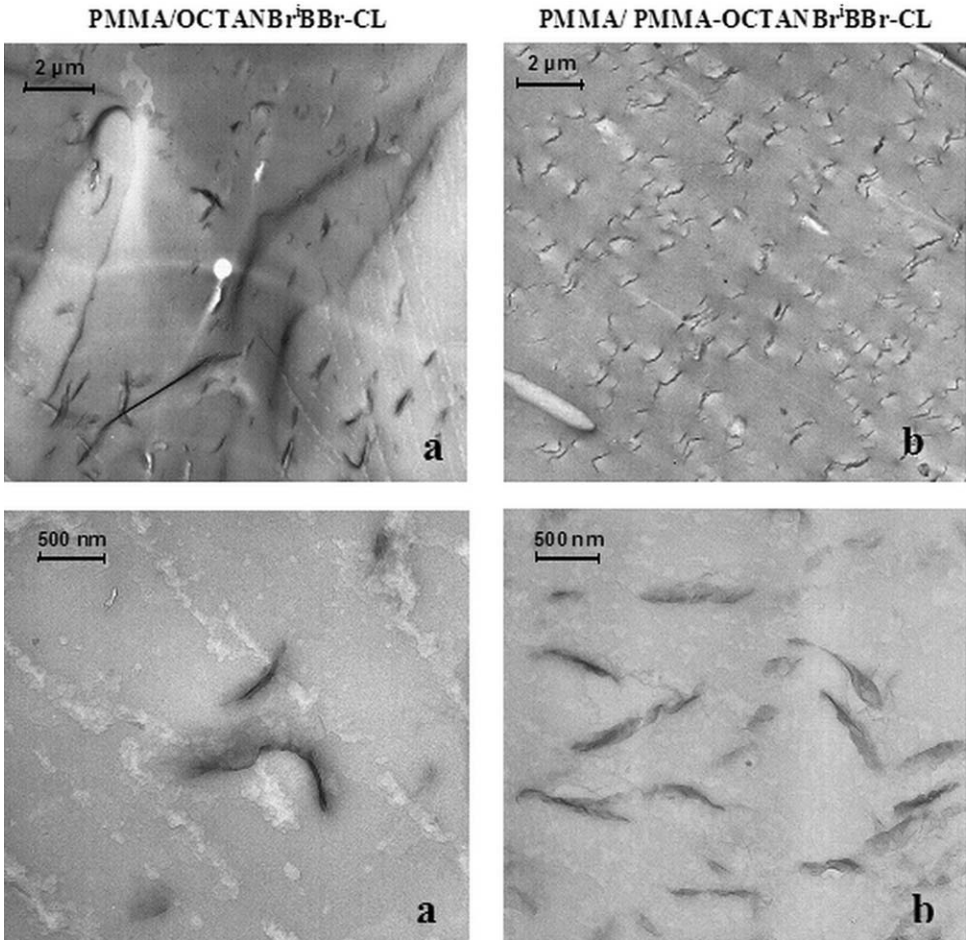

Figure 4 TEM micrographs for PMMA/OCTANBr^{i}BBr-CL and PMMA/PMMA-OCTANBr^{i}BBr-CL nanocomposites (3 wt % of inorganics).

shifted to higher angle value with an interlayer spacing value of 14.7Å. Indeed, as illustrated in Figure 3, the peak of the nanocomposite is situated between the peak of the clay before and after organo-modification. This decrease in the interlayer spacing from 20.9 to 14.7 Å (~ 6 Å) suggests a collapse of the platelets probably because of two combined effects: (a) the presence of bromide groups may increase the interaction energy of clay and modifier, leading to relatively lower interaction energies between the polymer and the organomodified nanoclay, (b) the lower degradation temperature of the intercalant (~ 200°C), which is in the range of the processing temperature leading to a stack up of the silicate layers. As a result, no evidence of exfoliation is concluded as confirmed by TEM [Fig. 4(a)]. This result is in agreement with literature,[41–45] where such a clay interlayer collapse has been observed and accounted for by some rearrangement of the used intercalants triggered by processing at high temperature.

Nanocomposites obtained via masterbatch process

The diffractogram of PMMA/PMMA-OCTAN-Br^{i}BBr-CL (Fig. 3) attests for some level of clay delamination (at least destructuration of the clay tactoids). The diffraction peak shifts to a much lower angle ($2\theta = 2.04°$; $d_{001} = 43.27$ Å). This result indicates that the PMMA segments grafted on the intercalant through ATRP may increase the interaction energy between the surface-grafted clay and the matrix and favor the insertion of further macromolecules into the clay galleries. It is worth noting that low intensity diffraction peaks are also observed at $2\theta = 5°$ and 6° and could be again attributed to degradation of some intercalant molecules along with the high temperature melt processing.

The representative TEM images [Fig. 4(b) at high and low magnifications] of PMMA/PMMA-OCTAN-Br^{i}BBr-CL nanocomposites display a homogeneous dispersion of nanoplatelets throughout the matrix without any visible remaining stacks. They attest for a high extent of exfoliation in case of the nanocomposite as produced starting from the preformed nanohybrid. These observations thus confirm that the masterbatch approach leads to much finer dispersion of the silicate nanoplatelets in the PMMA matrix.

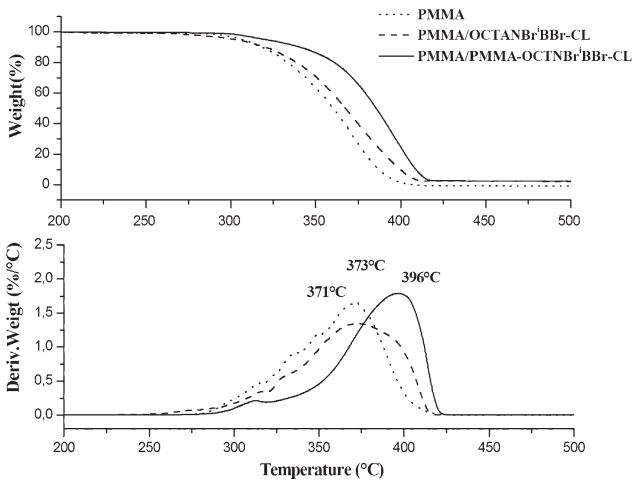

Figure 5 Thermogravimetric analysis curves of PMMA, PMMA/OCTANBr^{i}BBr-CL, and PMMA/PMMA-OCTANBr^{i}BBr-CL with 3 wt % of inorganics in air at 20 K/min.

Thermal properties

Thermogravimetric analysis

The effect of nanoclay dispersion on the PMMA thermal stability was assessed by thermogravimetric analysis (TGA) with a heating rate of 20 K/min under oxidative and inert atmosphere.[46] Figure 5 shows the thermogravimetric curves of PMMA, PMMA/OCTANBr^{i}BBr-CL, and PMMA/PMMA-OCTANBr^{i}BBr-CL (nano)composites as recorded under air flow. As shown in Figure 5, the maximum degradation temperature of pristine PMMA is located at 378°C under helium versus 370°C in air. This maximum is recorded at 389°C under helium versus 373°C in air for the PMMA/OCTANBr^{i}BBr-CL direct blend, thus showing a limited delay of weight loss between the degradation temperature in air and in helium. The use of the PMMA-OCTANBr^{i}BBr-CL nanohybrid as masterbatch triggers the most important delay of weight loss under oxidative conditions: with respect to unfilled PMMA the maximum degradation temperature is only increased by 3°C in case of PMMA/OCTANBr^{i}BBr-CL direct blend, while it is increased by about 26°C for PMMA/PMMA-OCTANBr^{i}BBr-CL nanocomposites. Thus it comes out that the degradation behavior of nanocomposite produced starting from the PMMA-OCTANBr^{i}BBr-CL nanohybrid is almost similar in air and in helium (Fig. 6). Such a behavior has been

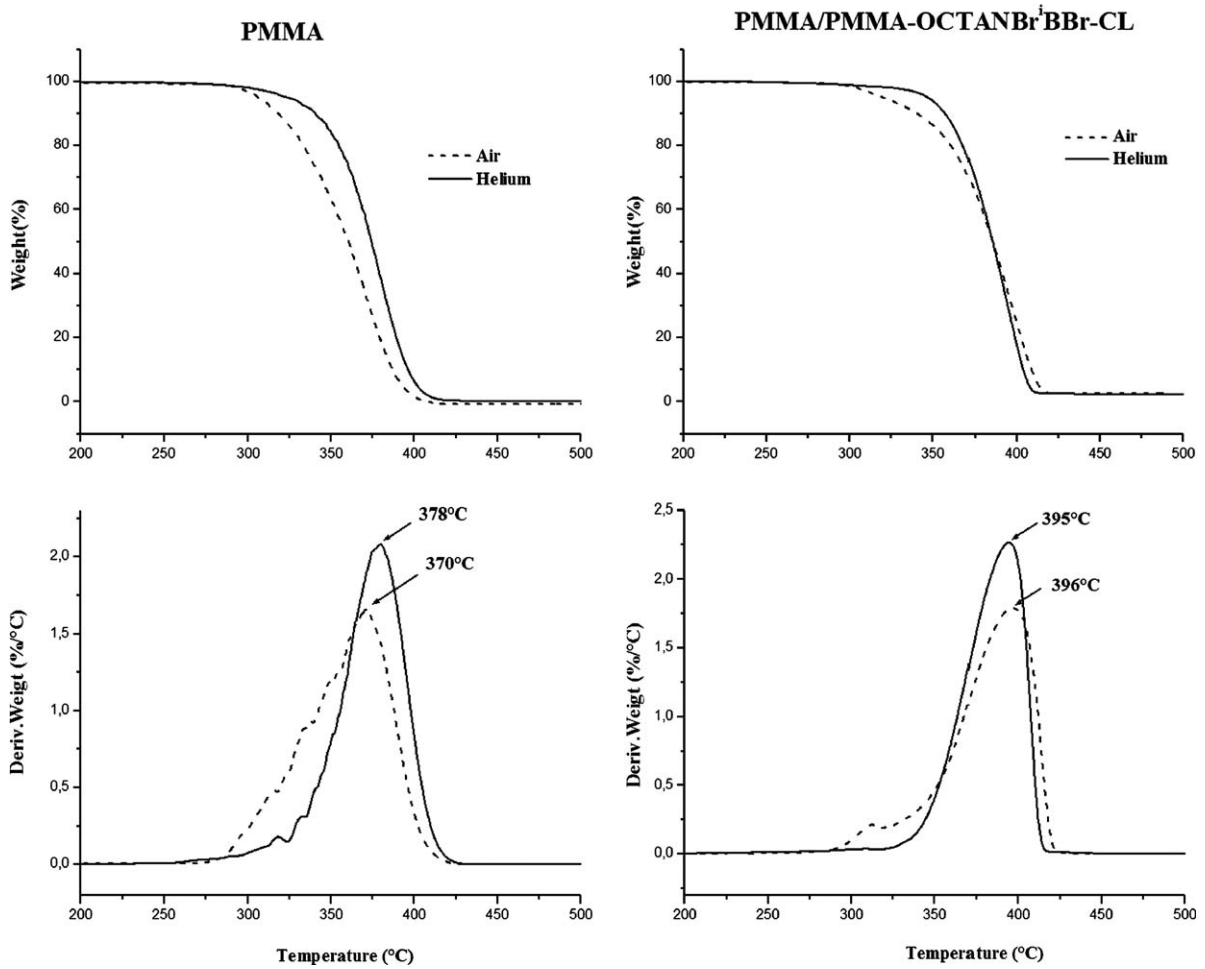

Figure 6 Thermogravimetric analysis curves of PMMA and PMMA/PMMA-OCTANBr^{i}BBr-CL with 3 wt % of inorganics in air (---) and in helium (—) at 20 K/min.

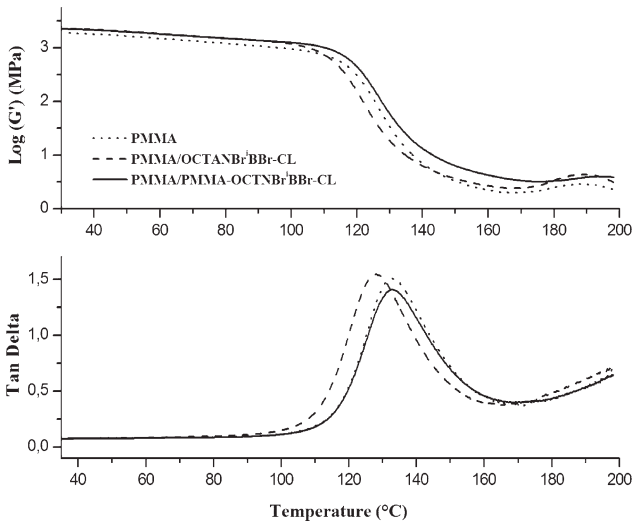

Figure 7 DMTA traces of pristine PMMA and PMMA nanocomposites recorded in the dual cantilever mode (1 Hz, 3 K/min).

assigned to the so-called "nano-effect."[35,46,47] Indeed, homogeneously dispersed organoclay are known to behave as physical barriers that are able to inhibit or at least refrain the diffusion of both the volatile thermo-oxidation products to the gas phase and oxygen from the gas phase to the polymer and limits then the degradation of polymer matrix. This effect is in accordance with the morphology of the PMMA/PMMA-OCTANBr^{i}BBr-CL nanocomposites with clay sheets finely dispersed as evidenced by TEM. In conclusion, PMMA-clay nanocomposites prepared by the nanohybrid-based masterbatch process present the most improved properties in terms of thermal degradation recorded under both oxidative and inert atmospheres. Accordingly, impermeability, i.e., gas barrier properties, of the resulting nanocompositions (not investigated in the present contribution) can be expected to be improved as well.

Dynamic mechanical thermal analysis

The impact of this new type of nanofiller on the viscoelastic properties of PMMA has been investigated using dynamic mechanical analysis. Figure 7 shows the temperature dependence of the storage modulus and tan δ of PMMA and two corresponding nanocomposites. The storage modulus is not affected by the presence of the filler, whatever the preparation method. Only slight increase due to the presence of the filler is detected. The glass transition temperature determined by the maximum of the tan δ peak is decreased for the microcomposite. This phenomenon is generally observed when interaction between nanofiller and polymeric matrix is lost.[48–50]

Clearly, this new method, leading to more dispersed nanoclays in PMMA does not affect the viscoelastic properties of PMMA.

Fire testing

To shed some light on the flame retardancy properties of PMMA-based nanocomposites, a simple visual fire testing has been performed (Figure 8). It consists in burning two specimens (unfilled PMMA and PMMA/PMMA-OCTANBr^{i}BBr-CL nanocomposite) and recording their combustion behavior. As expected, the unfilled PMMA sample burns with continuous dripping during the whole process. The combustion is achieved after 100 s. It is worth noting that the nanocomposite obtained by direct melt blending shows a similar combustion behavior (not

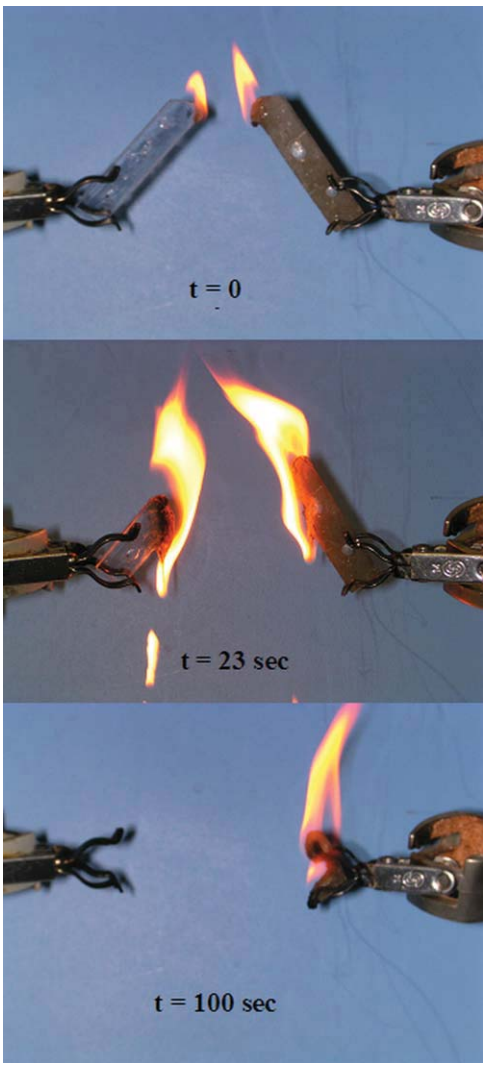

Figure 8 Qualitative fire behavior test of unfilled PMMA (left) and PMMA/PMMA-OCTANBr^{i}BBr-CL nanocomposite (right) with 3 wt % of inorganics. [Color figure can be viewed in the online issue, which is available at wileyonlinelibrary.com.]

presented here). Interestingly enough, the PMMA/PMMA-OCTANBr^{i}BBr-CL nanocomposite prepared via the masterbatch process burns more slowly with extinguishment occurring after 148 s. These observations reveal the interest of the PMMA-grafted clay nanohydrid used as masterbatch for the preparation of PMMA-based nanocomposites with enhanced flame retardant properties, actually in agreement with the previously discussed thermogravimetric analyses.

CONCLUSIONS

PMMA/layered silicate nanocomposites were prepared by two processes: a simple blending of organomodified clay and PMMA in the melt and via masterbatch approach. The clay platelets were first organically modified with OCTANBr^{i}BBr, a functionalized ammonium able to initiate the ATRP of MMA monomer. To promote clay dispersion and nanoplatelet delamination, a highly filled PMMA-OCTANBr^{i}BBr-CL (containing 31 wt % of inorganics), previously synthesized by ATRP, was used as masterbatch to obtain nanocomposites with 3 wt % of inorganics. This methodology permits to achieve an exfoliated nanostructure as evidenced by XRD and TEM analyses of these nanomaterials. Their properties are improved in terms of thermal stability and flame retardant properties without affecting the viscoelastic properties. This contribution underlines the interest of using the nanohybrid-based masterbatch route to optimize the dispersion state of silicate nanolayers in PMMA and enhance their final thermal properties.

CIRMAP is grateful to the 'Région Wallonne' and European Community (FSE, FEDER) in the frame of Phasing Out financing of Materia Nova. D. Lerari thanks University of Mons for her research stay in Mons, Belgium.

References

1. Sahoo, P. K.; Samal, R. Polym Degrad Stab 2007, 92, 1700.
2. Kumar, S.; Jog, J. P.; Natarajan, U. J Appl Polym Sci 2003, 89, 1186.
3. Gross, S.; Camozzo, D.; Noto, V.; Armelao, L.; Tondello, E. Eur Polym Mater 2007, 43, 673.
4. Mark, H. F.; Bikales, N. M.; Overberger, C. G.; Menges, G. Encyclopedia of Polymer Science and Engineering; Wiley: New York, 1985.
5. Ash, B. J.; Rogers, D. F.; Wiegand, C. J.; Schadler, L. S.; Siegel, R. W.; Benicewicz, B. C. Polym Compos 2004, 23, 1014.
6. Horikawa, A.; Yamaguchi, K.; Inoue, M.; Fujii, T.; Arai, K. Mater Sci Eng 1996, 348, 217.
7. Thander, A.; Mallik, B. Solid State Commun 2002, 121, 159.
8. Lepoittevin, B.; Pantoustier, N.; Devalckenaere, M.; Alexandre, M.; Kubies, D.; Calberg, C.; Jérôme, R.; Dubois, Ph. Macromolecules 2002, 35, 8385.
9. Morlat-Therias, S.; Mailhot, B.; Gonzalez, G.; Gardette, J. Chem Mater 2005, 17, 1072.
10. Alexandre, M.; Dubois, Ph. Mater Sci Eng C 2000, R28, 1.
11. Ray, S. S.; Okamoto, M. Prog Polym Sci2003, 28, 1539.
12. Piner, R. D.; Xu, T. T.; Fisher, F. T.; Qiao, Y.; Ruoff, R. S. Langmuir 2003, 19, 7995.
13. Esfandiari, A.; Nazokdast, H.; Rashidi, A.; Yazdanshenas, M. E. J Appl Polym Sci 2008, 8, 545.
14. Giannelis, E. P.; Krishnamoorti, R.; Manias, E. Adv Polym Sci 1999, 138, 107.
15. Lagaly, G. Appl Clay Sci1999, 15, 1.
16. Fisher, H. Mater Sci Eng C 2003, 23, 763.
17. Shan, C.; Gu, Z.; Wang, L.; Li, P.; Song, G.; Gao, Z. J Appl Polym Sci 2010, 119, 1185.
18. Sterky, K.; Jacobsen, H.; Jakubowicz, I.; Yarahmadi, N.; Hjertberg, T. Eur Polym J 2010, 46, 1203.
19. Sterky, K.; Hjertberg, T.; Jacobsen, H. Polym Degrad Stab 2009, 94, 1564.
20. Meneghetti, P.; Qutubuddin, S. Langmuir2004, 20, 3424.
21. Yang, Y.; Liu, L.; Zhang, J.; Li, C.; Zhao, H. Langmuir 2007, 23, 2867.
22. Khaled, S. M.; Sui, R.; Charpentier, P.; Rizkalla, A. S. Langmuir 2007, 23, 3988.
23. Cui, L.; Naresh, H.; Tarte, S. I. W. Macromolecules 2008, 41, 4268.
24. Zhao, Q.; Samulski, E. T. Macromolecules 2005, 38, 7967.
25. Cui, L.; Naresh, H.; Tarte, I. W. Macromolecules 2009, 42, 8649.
26. Wang, D. Y.; Zhu, J.; Yao, Q.; Wilkie, C. A. Chem Mater 2002, 14, 3837.
27. Shen, Z.; Simon, G. P.; Cheng, Y. B. J Appl Polym Sci 2004, 92, 2101.
28. Kim, Y.; White, J. L. J Appl Polym Sci 2005, 96, 1888.
29. Salahuddin, N.; Shehata, M. Polymer 2001, 42, 8379.
30. Wheeler, P. A.; Wang, J.; Mathias, L. J. Chem Mater 2006, 18, 3937.
31. Benali, S.; Peeterbroeck, S.; Brocorens, P.; Monteverde, F.; Bonnaud, L.; Alexandre, M.; Lazzaroni, R.; Dubois, Ph. Eur Polym Mater 2008, 44, 1673.
32. Broekaert, C.; Peeterbroeck, S.; Benali, S.; Monteverde, F.; Bonnaud, L.; Alexandre, M; Dubois, Ph. Eur Polym Mater 2007, 43, 4160.
33. Brocorens, P.; Benali, S.; Broekaert, C.; Monteverde, F.; Miltner, H. E.; Van Mele, B.; Alexandre, M.; Dubois, Ph.; Lazzaroni, R. Langmuir 2008, 24, 2072.
34. Urbanczyk, L.; Calberg, C.; Benali, S.; Bourbigot, S.; Espuche, E.; Gouanve, F.; Dubois, Ph.; Germain, A.; Jérôme, C.; Detrembleur, C.; Alexandre, M. J Mater Chem 2008, 18, 4623.
35. Benali, S.; Olivier, A.; Brocorens, P.; Bonnaud, L.; Alexandre, M.; Bourbigot, S.; Espuche, E.; Gouanve, F.; Lazzaroni, R.; Dubois, Ph. Adv Mater Sci Eng 2008, ID 394235, 1.
36. Lepoittevin, B.; Pantoustier, N.; Devalckenaere, M.; Alexandre, M.; Calberg, C.; Jérôme, R.; Henrist, C.; Rulmont, A.; Dubois, Ph. Polymer 2003, 44, 2033.
37. Paul, M. A.; Alexandre, M.; Degée, P.; Calberg, C.; Jérôme, R.; Dubois, Ph. Macromol Rapid Commun 2003, 24, 561.
38. Paul, M. A.; Delcourt, C.; Alexandre, M.; Degée, M.; Monteverde, F.; Rulmont, A.; Dubois, Ph. Macromol Chem Phys 2005, 206, 484.
39. Pollet, E.; Delcourt, C.; Alexandre, M.; Dubois, Ph. Eur Polym Mater 2006, 42, 1330.
40. Lerari, D.; Peeterbroeck, S.; Benali, S.; Benaboura, A.; Dubois, Ph. Polym Int 2010, 59, 71.
41. Benali, S.; Peeterbroeck, S.; Larrieu, J.; Laffineur, F.; Pireaux, J.; Alexandre, M.; Dubois, Ph. J Nanosci Nanotechnol2008, 8, 1707.
42. Rohlmann, C. O.; Fernanda Horst, M.; Quinzani, L. M.; Failla, M. D. Eur Polym Mater 2008, 44, 2749.
43. Park, C.; Kim, M. H.; Park, O. Polymer 2004, 45, 1267.

44. Yoon, J. T.; Jo, W. H.; Lee, M. S.; Ko, M. B. Polymer 2001, 42, 329.
45. Perrin-Sarazin, F.; Ton-That, M.; Bureau, M.; Denault, J. Polymer 2005, 46, 11624.
46. Zanetti, M.; Camino, G.; Thomann, R.; Mülhaup, R. Polymer 2001, 42, 4501.
47. Laachachi, A.; Ruch, D.; Addiego, F.; Ferriol, M.; Cochez, M.; Lopez Cuesta, J. M. Polym Degrad Stab 2009, 94, 670.
48. Meneghetti, P.; Qutubuddin, S. Thermochim Acta 2006, 442, 74.
49. Wei'an, Z.; Xiaofeng, S.; Yu, L.; Yue'e, F. Radiat Phy Chem 2003, 67, 651.
50. Ash, B. J.; Schadler, L. S.; Siegel, R. W. Mater Lett 2002, 55, 83.